Quantitative Molecular Level Understanding of Ethoxysilane at Poly(dimethylsiloxane)/Polymer Interfaces

ARTICLE *in* LANGMUIR · DECEMBER 2012

Impact Factor: 4.46 · DOI: 10.1021/la3041727 · Source: PubMed

2 AUTHORS, INCLUDING:

Chi Zhang
Purdue University
33 PUBLICATIONS **222** CITATIONS

SEE PROFILE

Langmuir

Article

pubs.acs.org/Langmuir

Quantitative Molecular Level Understanding of Ethoxysilane at Poly(dimethylsiloxane)/Polymer Interfaces

Chi Zhang and Zhan Chen*

Department of Chemistry, University of Michigan, Ann Arbor, Michigan 48109, United States

ABSTRACT: Because of the wide applications of silicone adhesives, it is important to study adhesion mechanisms of silicone elastomers to polymers. Adhesion properties are believed to be directly related to the molecular structures at the adhesive/substrate interfaces. To improve adhesion, adhesion promoters such as silanes are commonly used to modify the interfacial structures. It is difficult to study buried interfacial molecular structures between two materials *in situ* using conventional analytical techniques. In this study, sum frequency generation (SFG) vibrational spectroscopy was used to investigate molecular structures at buried silicone/poly(ethylene terephthalate) (PET) interfaces. Environmental-friendly epoxysilanes including (3-glycidoxypropyl)-triethoxysilane (γ-GPES), (3-glycidoxypropyl)methyldiethoxysilane (γ-GPDES), and (3-glycidoxypropyl)dimethylethoxysilane (γ-GPDMES) and their mixtures with methylvinylsiloxanol (MVS) were used as adhesion promoters to modify silicone adhesion properties to PET. Various PET/silane, PET/uncured silicone, and PET/cured silicone interfaces were examined. The interfacial structures deduced from SFG spectra were correlated to adhesion testing results. It was found that silane headgroup order at the polymer interfaces is an important factor for improving adhesion. The decrease of silane headgroup order due to chemical reaction and disordering of such groups at the polymer interfaces can be associated with improved adhesion. The molecular level understanding on polymer/adhesive interfacial structures helps to design and develop adhesion promoters and polymer adhesives with improved performance.

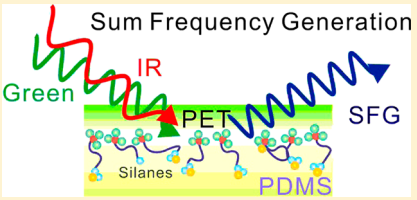

INTRODUCTION

Silicone-related products such as polydimethylsiloxane (PDMS) have many important applications and are widely used in industry. PDMS elastomers are very stable in various extreme environments and can be used in a very wide temperature range. Particularly, addition-cured PDMS materials exhibit good rheological properties, good biocompatibility, and excellent fouling-release properties with a simple and controllable curing process.[1,2] However, the adhesion between the addition-cured PDMS elastomers and polymers can be very weak due to the loss of intrinsic functional groups that are responsible for good adhesion. Many different methods to pretreat the substrate surfaces such as plasma treatment, corona discharge treatment, mechanical abrasion, or solvent cleaning followed by wet chemical etching were used to improve the adhesion strength.[3,4] Such pretreatments greatly increase the cost and are time-consuming. A different means to improve the PDMS adhesion which is more commercially attractive is to introduce adhesion promoters to the elastomer to make PDMS self-adhere to polymers.[4] Adhesion promoters are usually small molecules that typically employ as additives and can enhance adhesion at the substrate/adhesive interface. Many organosilanes have been developed as adhesion promoters, especially for silicone elastomer.[4−12] It is believed that these silane adhesion promoters modified the interfaces between the substrates and silicone elastomers. However, the detailed mechanism of how adhesion is improved has not been precisely understood at the molecular level due to the lack of appropriate techniques.

Many techniques have been applied to study adhesion involving PDMS materials.[13−16] The traditional way to study interfacial structures is to break the interface and examine the two resulting surfaces. This method may alter the original chemical structure that is responsible for good adhesion, and thus the results may not accurately reflect the interfacial chemistry. Therefore, it is important to develop a technique to investigate the molecular structures at a buried substrate/adhesive interface *in situ*.

Sum frequency generation (SFG) vibrational spectroscopy has been developed into a versatile technique to study surfaces and interfaces of different materials *in situ*.[17−24] SFG is a second-order nonlinear optical process, and SFG signals can only be generated from media with no inversion symmetry, e.g., surfaces and interfaces. SFG can study surfaces or interfaces which can be accessed by the laser beams and can provide the *in situ* capability for probing molecular structures at buried interfaces. SFG can detect the presence, coverage, and molecular orientation of surface or interfacial chemical groups *in situ*. The theory of SFG vibrational spectroscopy has been well developed[17,20,25−30] and will not be discussed in detail here. SFG has also been applied to study surfaces and interfaces of different materials experimentally, including polymers,[31−42] water,[18,43,44] biomolecules,[23,45−47] etc. In our group, we have used SFG to study polymer/air, polymer/liquid, and polymer/polymer interfaces.[35,39,48−51] Especially, we have used SFG to

Received: October 21, 2012
Revised: December 10, 2012
Published: December 15, 2012

investigate molecular behavior of silane adhesion promoters at different polymer interfaces.[52,53] Furthermore, we have extended our research by incorporating silanes to silicone elastomers to study the end-group effect[54] and headgroup effect[55] of these silanes in adhesion. It has been shown that the epoxy end groups can greatly enhance adhesion compared to other end groups, and the methoxy headgroups tend to order at the interfaces between PDMS and poly(ethylene terephthalate) (PET). The interfacial reaction during the curing process decreases the SFG signals generated from the methoxy group at the interface and leads to strong adhesion.[54]

Besides methoxysilanes (with methoxy headgroups), chloride silanes (with chloride headgroups) have also been used as adhesion promoters. The disadvantage of the above silanes is that in the adhesion promoting process they tend to release harmful methanol or corrosive hydrochloric acid, respectively.[10] To reduce negative environmental impact, silanes with ethoxy headgroups (ethoxysilanes) are used as adhesion promoters. In the adhesion promoting reaction, ethoxysilanes tend to release harmless ethanol molecules.[56] In this research, we studied three epoxysilanes with the same backbone and end group, but different headgroups at the buried interfaces between PDMS and PET. The mechanical adhesion test results show great differences in adhesion of different PDMS silane mixtures. In order to understand the molecular level mechanism of such differences, we used SFG to investigate the buried interfaces *in situ*. SFG results show that silane ethoxy headgroups segregate to the PDMS/PET interface and play an important role in adhesion. Quantitative analysis of the SFG results was correlated to the mechanical adhesion testing data to further understand the adhesion mechanism. Together with the results obtained from previous studies,[55] we can conclude that silane headgroups can greatly impact adhesion at the polymer/silicone interface.[4]

MATERIALS AND METHODS

Materials. The (3-glycidoxypropyl)triethoxysilane (γ-GPES), (3-glycidoxypropyl)methyldiethoxysilane (γ-GPDES), and (3-glycidoxypropyl)dimethylethoxysilane (γ-GPDMES) were purchased from Sigma-Aldrich. Methylvinylsiloxanol (MVS) and Sylgard 184 silicone elastomer kit were purchased from Dow Corning Corporation. The Sylgard 184 silicone elastomer was prepared by mixing the base and the curing agent with a 10:1 ratio. To incorporate silanes into PDMS, 1.5 wt % γ-GPES, 3.0 wt % 1:1 (w/w) γ-GPES/MVS mixture, 1.5 wt % γ-GPDES, 3.0 wt % 1:1 (w/w) γ-GPDES/MVS mixture, and 1.5 wt % γ-GPDMES, 3.0 wt % 1:1 (w/w) γ-GPDMES/MVS mixture were mixed homogeneously using a vortex mixer (Vortex-Genie 2T, Scientific Industries Inc.) into the silicone mixture before curing. When MVS was added, a SiH-functional PDMS was added to maintain a 1.5:1 SiH/vinyl molar ratio. The PDMS samples were cured in an oven at 140 °C for 120 min on d_4-PET surface. The samples were then stored at room temperature for 24 h before use. The aliphatic deuterated poly(ethylene terephthalate) (d_4-PET, M_n = 72 000) films were prepared by spin-coating the 2 wt % d_4-PET solution at 2500 rpm on fused silica right angle prisms. Fused silica prisms were obtained from Altos Photonics, Inc. The prisms were cleaned using concentrated sulfuric acid saturated with potassium dichromate overnight at 60 °C. The prisms were then rinsed using deionized water and dried with nitrogen gas before use. d_4-PET was obtained from Polymer Source, Inc., and was dissolved in 2-chlorophenol to form a 2 wt % solution. The molecular formulas of the materials used in this research are shown in Figure 1.

Adhesion Test. On the basis of the ASTM D3163 standard with some modifications, we carried out mechanical adhesion test of Sylgard 184 silicone elastomer to PET blocks using an Instron 5544 mechanical testing instrument. The testing geometry in the experiment

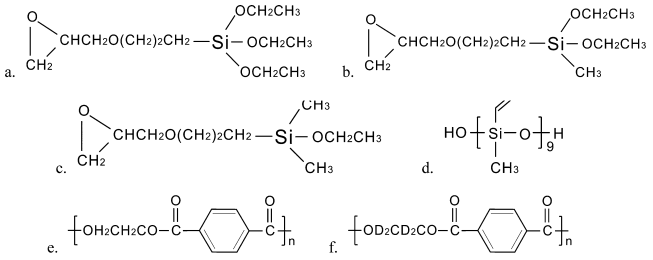

Figure 1. Chemical structures of silanes and polymers employed in the study: (a) (3-glycidoxypropyl)triethoxysilane (γ-GPES); (b) (3-glycidoxypropyl)methyldiethoxysilane (γ-GPDES); (c) (3-glycidoxypropyl)dimethylethoxysilane (γ-GPDMES); (d) methylvinylsiloxanol (MVS); (e) poly(ethylene terephthalate) (PET); (f) poly(ethylene terephthalate) with aliphatic chain deuterated (d_4-PET).

is 180° shear strength test (as shown in Figure 2). A PET sheet (Ertalyte) was cut into small pieces with the same size. The contact

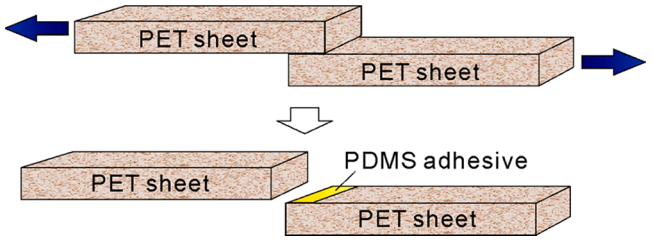

Figure 2. Adhesion test geometry for shear strength test. The top panel shows two test pieces adhered together by PDMS adhesive; the bottom panel shows that after the 180° shear test, two test pieces were pulled apart.

surface area of each PET test piece is 30.0 × 12.0 mm^2. The PET surfaces were sanded and cleaned using ethanol before use. Two PET pieces were attached by using different PDMS silane (with or without MVS) mixtures and cured at 140 °C for 120 min. Then the test pieces are stored at room temperature for 24 h. The PDMS adhesive thickness is about 0.5 mm. The bonded PET pieces were pulled apart at the room temperature with the pulling speed of 1.3 mm/min while the shear strength was measured. In this experiment, all the failures we observed are at the interfaces of PET and silicone elastomer (adhesive failure), not in the silicone elastomer bulk (cohesive failure).

SFG Experiment. The picosecond SFG system (from EKSPLA) used in this study was reported in previous publications.[35,52,54,55,57] Briefly, a frequency tunable mid-infrared (mid-IR) laser beam and a 532 nm visible laser beam were generated from a Nd:YAG laser system and overlapped at the sample interface spatially and temporally. The input laser pulses are both ~20 ps in time and 30 μJ (visible) and 100 μJ (mid-IR) in energy. The SFG experimental geometry is shown in Figure 3. SFG signal generated at the interface was collected by a monochromator together with a photomultiplier tube. SFG spectra in this study were collected in ssp (s-polarized sum frequency output, s-

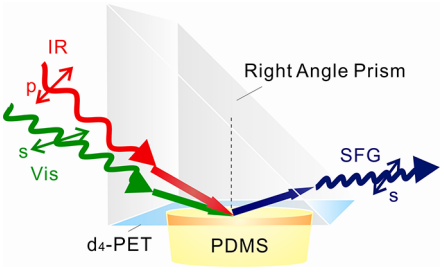

Figure 3. Experimental geometry used in the experiment.

dx.doi.org/10.1021/la3041727 | *Langmuir* 2013, 29, 610–619

polarized visible input, and p-polarized IR input) polarization combination. Each SFG spectrum presented here is the average of 10 spectra collected from the same sample but different spots. Several samples of the same type have been tested, and all spectra were reproducible.

Spectral Fitting of SFG. The SFG signal intensity can be expressed as

$$I_{SFG} \propto |\chi^{(2)}_{eff}|^2 I_{IR} I_{vis} \quad (1)$$

Here I_{IR} and I_{vis} are the input IR and visible beam intensities, respectively. $\chi^{(2)}_{eff}$ is the effective second-order nonlinear susceptibility of the interface, which can be written as

$$\chi^{(2)}_{eff} = \chi^{(2)}_{NR} + \sum_q \frac{A_q}{\omega_{IR} - \omega_q + i\Gamma_q} \quad (2)$$

In this expression, $\chi^{(2)}_{NR}$ is the nonresonant contribution from the sample. The resonant contribution can be modeled as a sum of Lorentzian peaks with signal strength or amplitude A_q, frequency ω_q, and line width Γ_q. In this paper, we used eq 2 to fit the SFG spectra to obtain resonant nonlinear susceptibility component of the material. The fitting results can be used to quantitatively compare and analyze SFG spectra detected from different interfaces.

RESULTS AND DISCUSSION

Adhesion Test Results. The adhesion test results for PDMS and PDMS silane mixtures with and without MVS adhere to PET using the 180° shear test are shown in Figure 4.

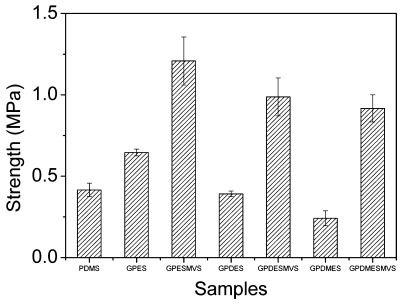

Figure 4. Adhesion test results of ethoxysilanes incorporated in PDMS adhesives adhere to PET. Samples from left to right: PDMS, γ-GPES, γ-GPES:MVS, γ-GPDES, γ-GPDES:MVS, γ-GPDMES, γ-GPDMES:MVS. Only a very small amount of silane or silane:MVS mixture was added to PDMS in these cases.

In the tests, five samples were prepared for each type, and therefore each experiment was reproduced five times. The results with error bars shown in Figure 4 are the averaged values with the standard deviations. Figure 4 shows clearly that silanes with different ethoxy headgroups exhibit different adhesion promotion behavior when incorporated into PDMS. Compared to PDMS alone, the γ-GPES tends to increase the adhesion to PET, γ-GPDES does not significantly alter the adhesion, and γ-GPDMES tends to decrease the adhesion. When MVS was added to the mixture together with silanes, all samples show substantially increased adhesion strength, while the measured strengths are γ-GPES:MVS > γ-GPDES:MVS > γ-GPDMES:MVS. These results indicate that silane ethoxy headgroups tend to improve the interfacial adhesion between PET and PDMS. The more ethoxy groups the silane has, the stronger adhesion its mixture with PDMS tends to have. It also shows that MVS can greatly improve the adhesion of silane PDMS mixtures to PET.

However, it is still unclear at the molecular level how silane headgroup can affect the adhesion and why MVS improves the adhesion. Silanes are mixed in the PDMS with very small fractions; whether they can segregate to the PET/PDMS interface is unknown. If they do segregate to the interface, it is still unknown whether they form certain order. It is well-known that on a silica substrate where hydroxyl groups are present, ethoxysilanes can interact with the substrate through a chemical reaction. Ethoxy headgroup reacts with the hydroxyl group to release an ethanol molecule while the rest of the silane molecule directly binds to the silica substrate to improve adhesion. However, it is not known whether ethoxysilanes will have a similar reaction with polymer (e.g., PET) surfaces and whether ethoxy headgroups can play a role to improve adhesion to polymer surfaces. Silane headgroups may also cross-link at the PET substrate surface through reaction with water molecule adsorbed in air.[8,10,58] MVS has hydroxyl groups which may play a role for improving silane headgroup reaction at the substrate surface to form cross-linking. However, the headgroup segregation and reaction evidence was never detected. In order to have a further understanding on the molecular behaviors of interfacial silanes and MVS, SFG was applied to investigate the buried PET/PDMS interfaces.

SFG Study on Interfaces of d_4-PET/Silanes and d_4-PET/Silane:MVS Mixtures. In order to avoid spectral confusion from the methylene stretch in PET backbone, d_4-PET was used in SFG experiments. SFG spectra collected from various d_4-PET/silane and d_4-PET/silane:MVS mixture interfaces are shown in Figure 5. At the d_4-PET/γ-GPES interface, three

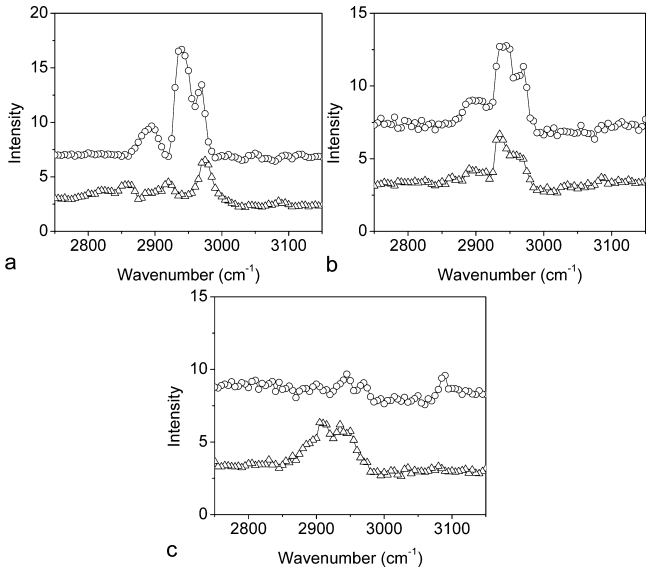

Figure 5. SFG ssp spectra of (a) d_4-PET/γ-GPES (bottom) and d_4-PET/γ-GPES:MVS mixture interfaces (top), (b) d_4-PET/γ-GPDES (bottom) and d_4-PET/γ-GPDES:MVS mixture interfaces (top), and (c) d_4-PET/γ-GPDMES (bottom) and d_4-PET/γ-GPDMES:MVS mixture interfaces (top).

peaks can be resolved at 2865, 2925, and 2975 cm^{-1}, which can be assigned to the methylene symmetric and asymmetric C−H stretches and the methyl (in ethoxy group) asymmetric C−H stretch, respectively. The peak at 2925 cm^{-1} may also have some contribution from the silane methyl Fermi resonance. However, since the peak center is slightly lower and no methyl symmetric stretching signal can be observed, it is more likely

dx.doi.org/10.1021/la3041727 | Langmuir 2013, 29, 610−619

that this peak is only or mainly contributed from the methylene asymmetric stretch. This indicates that both methylene and methyl groups in the silane molecule exhibit some order at the interface. At the d_4-PET/γ-GPES:MVS mixture interface, the Fermi resonance signal intensity from the methyl group (in the silane ethoxy headgroup) increased greatly at 2935 cm^{-1}. In addition to the asymmetric methyl stretching signal at 2972 cm^{-1}, another peak at around 2894 cm^{-1} was also observed and assigned to the methyl (in ethoxy) symmetric C−H stretch in silane. These results show that without MVS the silane headgroup tends to adopt some order at the d_4-PET interface. The stronger asymmetric C−H stretching signal indicates that the methyl groups in the ethoxy headgroup tilt more toward the surface.[35] The addition of MVS into the silane enhanced the ordering of silane methyl group (in the ethoxy headgroup) at the interface. The strong symmetric/Fermi resonance signals indicate that after the addition of MVS the methyl groups in ethoxy groups tend to stand up more at the interface.[35]

In the SFG spectrum collected from the d_4-PET/γ-GPDES interface, the methyl group signal at 2890, 2935, and 2975 cm^{-1} can also be detected. This shows that the silane headgroup adopts some order at the interface. After the addition of MVS to the silane, similar spectral features can be detected with stronger intensity. γ-GPDES has only two ethoxy headgroups; the methyl (in the ethoxy headgroup) symmetric stretch is weaker compared to γ-GPES, which has three ethoxy headgroups.

In the SFG spectrum collected from the d_4-PET/γ-GPDMES interface, the broad peak between 2900 and 2960 cm^{-1} should be contributed from the C−H stretching signals from the methyl headgroup (Si−CH_3) and ethoxy head groups (Si−OCH_2CH_3) of γ-GPDMES. After adding MVS to the silane, SFG spectrum collected from the d_4-PET/γ-GPDMES:MVS mixture interface shows three weak peaks, which is quite similar to the spectrum detected from the interface between pure MVS and d_4-PET.[55] The addition of MVS tends to decrease the coverage and/or order of γ-GPDMES silane headgroups at the PET interface.

These results show that MVS has different effects on the interactions between different silanes and d_4-PET. The addition of MVS increases the headgroup order at the d_4-PET/silane interfaces for γ-GPES and γ-GPDES silanes but decreases the methyl headgroup order at the γ-GPDMES/d_4-PET interface. To better understand the impact of silane and MVS on adhesion promoting, it is necessary to incorporate them into PDMS and study the structures at the PDMS/d_4-PET interfaces.

SFG Study on Interfaces of d_4-PET/Uncured PDMS Mixed with Silanes or Silane:MVS Mixtures. It has been reported that at d_4-PET/uncured PDMS interface only two weak peaks from Si−CH_3 symmetric and asymmetric modes at 2900 and 2960 cm^{-1} can be observed.[55] Here, SFG spectra were collected from d_4-PET/uncured PDMS interfaces when silane and silane:MVS mixtures were incorporated into PDMS. In order to quantitatively compare the silane ordering at interfaces, all SFG spectra shown in Figure 6 were fit using eq 2. The detailed fitting parameters are listed in Table 1.

At the d_4-PET/uncured PDMS γ-GPES mixture interface (Figure 6a), strong peaks at 2893, 2930, and 2965 cm^{-1} were detected, which can be assigned to the C−H symmetric stretching, Fermi resonance, and asymmetric stretching of methyl groups in ethoxy headgroups. The peak at 2893 and 2965 cm^{-1} may also have contributions from the methyl

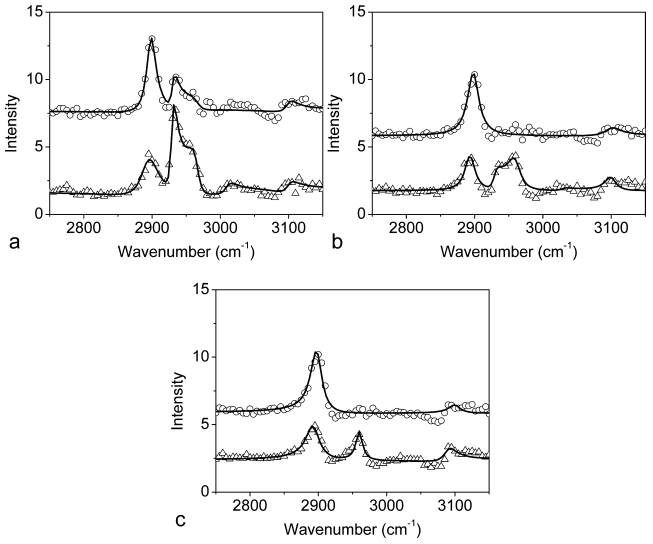

Figure 6. SFG spectra of (a) γ-GPES (bottom) and γ-GPES:MVS (top), (b) γ-GPDES (bottom) and γ-GPDES:MVS (top), and (c) γ-GPDMES (bottom) and γ-GPDMES:MVS (top) at d_4-PET/uncured PDMS interfaces under ssp polarization combination. The dots are experimental data, and lines are fitted results.

symmetric (at 2900 cm^{-1}) and asymmetric (at 2960 cm^{-1}) stretching signal of Si−CH_3 in PDMS. Compared to the d_4-PET/γ-GPES interface, the stronger SFG signals (especially the Fermi resonance signal which does not contain possible contributions from PDMS) indicated that uncured PDMS induced silane headgroups to be more ordered at the interface. The SFG spectrum was also collected from the d_4-PET/uncured PDMS γ-GPES:MVS mixture interface (Figure 6a). In this spectrum, the 2898 cm^{-1} signal could be assigned to the contribution from Si−CH_3 in PDMS and/or MVS. It might also have small contribution from the ethoxy methyl groups. Compared to the spectrum detected from the d_4-PET/uncured PDMS γ-GPES mixture interface, this symmetric C−H stretching contribution increased (signal strength from 1.52 to 2.31). However, both Fermi resonance and asymmetric C−H stretching peaks became weaker (signal strength from 1.85 and 1.33 to 1.04 and 0.51). Since the increased signal is not mainly contributed from the ethoxy methyl groups, but the decreased signals are mainly generated from the ethoxy methyl groups, we believe that the presence of MVS reduces γ-GPES ethoxy headgroup ordering at the d_4-PET/uncured PDMS interface.

At the d_4-PET/uncured PDMS γ-GPDES mixture interface (Figure 6b), three peaks of the methyl group can also be detected at 2892, 2931, and 2964 cm^{-1} from ethoxy headgroups. The 2892 and 2964 cm^{-1} signal may also contain contributions from the PDMS Si−CH_3 symmetric and asymmetric stretching. The 2931 cm^{-1} Fermi resonance signal is clearly weaker compared to the d_4-PET/uncured PDMS γ-GPES interface case (signal strength of 0.90 compared to 1.85). After the addition of MVS to the system, SFG spectrum at the interface (Figure 6b) shows only a strong peak at 2898 cm^{-1} (signal strength 2.17), which could be mainly from Si−CH_3 in PDMS or MVS. As the d_4-PET/uncured PDMS with γ-GPES interface discussed above, here the addition of MVS reduces the ethoxy group interfacial segregation/ordering.

The SFG spectrum collected from the d_4-PET/uncured PDMS γ-GPDMES mixture interface (Figure 6c) has two major

dx.doi.org/10.1021/la3041727 | Langmuir 2013, 29, 610−619

Table 1. Fitting Results of Figure 6

material (uncured)	ω_θ (cm^{-1})	$A_{q,ssp}$	Γ_θ (cm^{-1})	$\lvert A_{q,ssp}/\Gamma_q \rvert$	assignment
γ-GPES	2893	23.5 ± 1.0	15.5 ± 0.9	1.52 ± 0.11	$-CH_3$(s)
	2930	10.0 ± 0.6	5.4 ± 0.4	1.85 ± 0.18	$-CH_3$(s) Fermi
	2965	−13.0 ± 0.7	9.8 ± 0.4	1.33 ± 0.09	$-CH_3$(as)
γ-GPES:MVS	2898	19.6 ± 1.0	8.5 ± 0.5	2.31 ± 0.18	$-CH_3$(s)
	2931	5.7 ± 0.5	5.5 ± 0.4	1.04 ± 0.12	$-CH_3$(s) Fermi
	2966	−6.5 ± 0.4	12.8 ± 1.0	0.51 ± 0.05	$-CH_3$(as)
γ-GPDES	2893	14.5 ± 1.5	9.0 ± 1.2	1.61 ± 0.27	$-CH_3$(s)
	2931	7.0 ± 1.0	7.8 ± 0.7	0.90 ± 0.15	$-CH_3$(s) Fermi
	2964	−18.4 ± 0.9	11.8 ± 0.5	1.56 ± 0.10	$-CH_3$(as)
γ-GPDES:MVS	2898	21.7 ± 1.2	10.0 ± 0.7	2.17 ± 0.19	$-CH_3$(s)
γ-GPDMES	2893	20.5 ± 1.7	12.8 ± 1.3	1.60 ± 0.21	$-CH_3$(s)
	2960	−9.0 ± 0.8	6.0 ± 0.3	1.50 ± 0.15	$-CH_3$(as)
γ-GPDMES:MVS	2898	21.7 ± 1.6	10.2 ± 0.9	2.13 ± 0.24	$-CH_3$(s)

peaks at 2893 and 2960 cm^{-1} due to the C−H symmetric and asymmetric stretching signals of the methyl groups in the ethoxy headgroups. They may also contain some small contributions of the PDMS Si−CH_3 symmetric and asymmetric stretching. This is different from the spectrum detected from the d_4-PET/γ-GPDMES interface, indicating that the uncured PDMS influences the interfacial structure of γ-GPDMES. After the addition of MVS to the mixture (Figure 6c), the SFG spectrum at the interface has a strong peak at 2898 cm^{-1} (signal strength 2.13), which may be due to the Si−CH_3 group in MVS and PDMS.

In all the spectra shown in Figure 6, the C−H stretching signal from the phenyl ring in d_4-PET can be seen (~3100 cm^{-1}). Since the peak at ~2890 and ~2960 cm^{-1} may have some contribution from PDMS and MVS, it is difficult to quantitatively compare such peaks in Table 1. However, silane headgroup ordering can be compared using the Fermi resonance peak at ~2930 cm^{-1}, which can only be contributed from the ethoxy methyl group. The spectral fitting results for the peak ~2930 cm^{-1} shown in Table 1 demonstrate that the ethoxy headgroups in the ethoxysilane tend to order at the interfaces between d_4-PET and uncured PDMS. The addition of MVS greatly reduced interfacial segregation/order of these ethoxy headgroups at the d_4-PET/uncured PDMS interfaces. The results indicate clearly that PDMS can affect the interfacial structures of silanes and silane:MVS mixtures. MVS also has different effects on silane adhesion promoters at d_4-PET/PDMS interfaces. But overall, it tends to decrease the silane ethoxy headgroup ordering at such interfaces, which may be due to some interfacial chemical reaction or entanglement.

SFG Study on Interfaces of d_4-PET/Cured PDMS Mixed with Silanes or Silane:MVS Mixtures. SFG spectra were collected from the d_4-PET/cured PDMS mixed with silane or silane:MVS mixture interfaces and were fit (Figure 7). The detailed fitting parameters are listed in Table 2. The SFG spectrum collected from the d_4-PET/PDMS γ-GPES mixture interface after curing (Figure 7a) shows a very strong methyl headgroup Fermi resonance peak at 2930 cm^{-1} (signal strength 4.68). The weak peak at 2890 cm^{-1} was also observed (signal strength 1.31), attributed to the symmetric C−H stretches of methyl group (in ethoxy headgroup) and possibly methyl groups in PDMS. The methyl asymmetric stretch exhibits a shoulder at 2965 cm^{-1} in the spectrum. This indicates that methyl groups in ethoxy headgroups are quite ordered at the interface. After the addition of MVS to the system, the SFG spectrum collected from the d_4-PET/cured PDMS γ-GPES:MVS mixture interface (Figure 7a) showed that the intensity of the peak at 2930 cm^{-1} decreased (signal strength from 4.68 to 2.55). Therefore, the addition of MVS changed the silane headgroups at the cured PDMS interfaces and decreased silane headgroup orders.

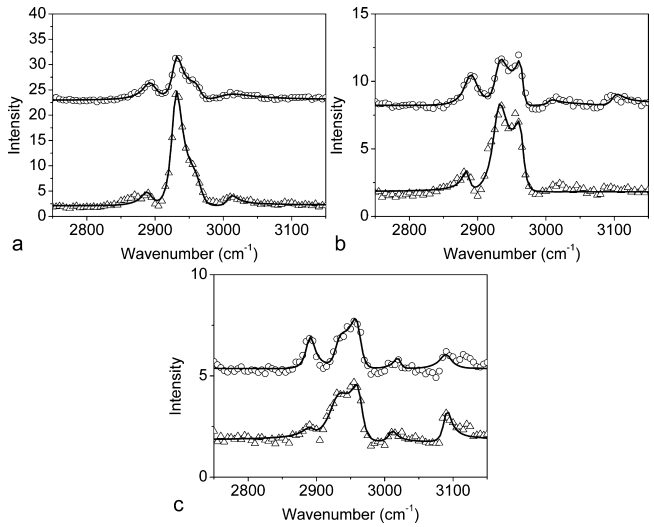

Figure 7. SFG spectra of (a) γ-GPES (bottom) and γ-GPES:MVS (top), (b) γ-GPDES (bottom) and γ-GPDES:MVS (top), and (c) γ-GPDMES (bottom) and γ-GPDMES:MVS (top) at d_4-PET/cured PDMS interfaces under ssp polarization combination. The dots are experimental data, and lines are fitted results.

The SFG spectrum collected from the d_4-PET/cured PDMS γ-GPDES mixture interface (Figure 7b) has three methyl peaks at 2890, 2930, and 2964 cm^{-1} from ethoxy headgroups. Peaks at 2890 and 2964 cm^{-1} may also have contributions from the PDMS methyl group. At this interface, silane headgroups also show some order at the interfaces similar to the γ-GPES case discussed above. After the addition of MVS to the mixture (Figure 7b), the SFG spectrum has similar features, but signal strengths are different (signal strengths changed from 0.91, 2.53, 2.24 to 1.42, 1.42, 1.61, respectively). Compared to the γ-GPES case, the SFG signal intensities are weaker. Silane headgroup order decrease after adding MVS was still observed by comparing peaks at 2930 cm^{-1}.

At the d_4-PET/cured PDMS γ-GPDMES mixture interface after curing (Figure 7c), three methyl peaks in ethoxy headgroups were also detected. PDMS may also contribute to methyl symmetric and asymmetric signals at 2890 and 2964

dx.doi.org/10.1021/la3041727 | Langmuir 2013, 29, 610−619

Table 2. Fitting Results of Figure 7

material (cured)	ω_q (cm^{-1})	$\lvert A_{q,ssp}\rvert$	Γ_q (cm^{-1})	$\lvert A_{q,ssp}/\Gamma_q\rvert$	assignment
γ-GPES	2890	13.2 ± 1.2	10.1 ± 1.0	1.31 ± 0.18	$-CH_3$(s)
	2930	44.9 ± 0.9	9.6 ± 0.2	4.68 ± 0.14	$-CH_3$ (Fermi)
	2965	−26.0 ± 1.0	12.8 ± 0.7	2.03 ± 0.14	$-CH_3$(as)
	3010	12.9 ± 1.8	9.4 ± 2.0	1.37 ± 0.35	−epoxy
γ-GPES:MVS	2893	21.0 ± 1.9	13.1 ± 1.2	1.60 ± 0.21	$-CH_3$(s)
	2930	23.7 ± 1.0	9.3 ± 0.4	2.55 ± 0.15	$-CH_3$ (Fermi)
	2964	−20.3 ± 1.3	10.1 ± 0.5	2.01 ± 0.16	$-CH_3$(as)
	3005	31.6 ± 3.0	29.9 ± 3.5	1.06 ± 0.16	−epoxy
γ-GPDES	2885	5.8 ± 0.9	6.4 ± 1.2	0.91 ± 0.22	$-CH_3$(s)
	2930	32.7 ± 1.6	12.9 ± 0.8	2.53 ± 0.20	$-CH_3$ (Fermi)
	2964	−17.9 ± 1.2	8.0 ± 0.2	2.24 ± 0.16	$-CH_3$(as)
γ-GPDES:MVS	2890	17.9 ± 1.5	12.6 ± 1.3	1.42 ± 0.19	$-CH_3$(s)
	2930	15.3 ± 1.7	10.8 ± 1.1	1.42 ± 0.21	$-CH_3$ (Fermi)
	2964	−9.0 ± 0.8	5.6 ± 0.3	1.61 ± 0.17	$-CH_3$(as)
	3005	3.7 ± 1.5	8.5 ± 5.0	0.44 ± 0.31	−epoxy
γ-GPDMES	2893	3.1 ± 0.8	9.8 ± 2.0	0.32 ± 0.10	$-CH_3$ (s)
	2930	29.3 ± 1.4	18.6 ± 1.0	1.58 ± 0.11	$-CH_3$ (Fermi)
	2963	−17.6 ± 0.9	9.8 ± 0.3	1.80 ± 0.11	$-CH_3$(as)
	3010	−5.4 ± 0.2	8.0 ± 0.4	0.68 ± 0.04	−epoxy
γ-GPDMES:MVS	2890	9.8 ± 1.1	8.1 ± 1.1	1.21 ± 0.21	$-CH_3$(s)
	2930	8.9 ± 1.0	10.8 ± 1.2	0.82 ± 0.13	$-CH_3$ (Fermi)
	2961	−13.1 ± 1.2	9.4 ± 0.4	1.39 ± 0.14	$-CH_3$(as)
	3010	−3.9 ± 0.6	6.0 ± 1.1	0.65 ± 0.16	−epoxy

Table 3. Fitting Result Summary from Tables 1 and 2

	symmetric (s)	Fermi (F)	asymmetric (as)	(s) + (F) + (as)
γ-GPES (uncured)	1.52 ± 0.11	1.85 ± 0.18	1.33 ± 0.09	4.70 ± 0.23
γ-GPES (cured)	1.31 ± 0.18	4.68 ± 0.14	2.03 ± 0.14	8.02 ± 0.27
γ-GPES:MVS (uncured)	2.31 ± 0.18	1.04 ± 0.12	0.51 ± 0.05	3.86 ± 0.22
γ-GPES:MVS (cured)	1.60 ± 0.21	2.55 ± 0.15	2.01 ± 0.16	6.16 ± 0.30
γ-GPDES (uncured)	1.61 ± 0.27	0.90 ± 0.15	1.56 ± 0.10	4.07 ± 0.32
γ-GPDES (cured)	0.91 ± 0.22	2.53 ± 0.20	2.24 ± 0.16	5.68 ± 0.34
γ-GPDES:MVS (uncured)	2.17 ± 0.19			2.17 ± 0.19
γ-GPDES:MVS (cured)	1.42 ± 0.19	1.42 ± 0.21	1.61 ± 0.17	4.45 ± 0.33
γ-GPDMES (uncured)	1.60 ± 0.21		1.50 ± 0.15	3.10 ± 0.26
γ-GPDMES (cured)	0.32 ± 0.10	1.58 ± 0.11	1.80 ± 0.11	3.70 ± 0.18
γ-GPDMES:MVS (uncured)	2.13 ± 0.24			2.13 ± 0.24
γ-GPDMES:MVS (cured)	1.21 ± 0.21	0.82 ± 0.13	1.39 ± 0.14	3.42 ± 0.28

cm^{-1}. Silane headgroups also have some order at the interfaces similar to the other two cases. After the addition of MVS to the mixture (Figure 7c), the SFG spectrum has similar features, but signals change intensities (from 0.32, 1.58, 1.80 to 1.21, 0.82, 1.39), similar to other two cases. Comparing the 2930 cm^{-1} Fermi resonance peak from the methyl headgroup, MVS also decreases the order of methyl functional groups at the d_4-PET/cured PDMS γ-GPDMES mixture interfaces, but such a change is smaller compared to the other two cases.

Correlation between Adhesion Test Results and Quantitative SFG Spectra. For comparison purpose, Table 3 summarizes the fitting results of the SFG signals contributed by the symmetric methyl stretch, Fermi resonance, and the asymmetric methyl stretch as well as the sum of all the above three SFG signals detected from the uncured and cured samples. As discussed above, the methyl group Fermi resonance signal at 2930 cm^{-1} does not have contributions from PDMS and MVS. Therefore, in order to quantitatively compare silane methyl headgroup ordering at different interfaces, we will compare Fermi resonance signals for all the cases. By using the detailed data analysis, we hope to understand the effects of the curing process and the addition of MVS on adhesion. To correlate SFG results to adhesion data, we list the signal strength differences of the Fermi resonance peaks and the adhesion testing data in Table 4.

Table 4 shows that the curing process tends to increase the silane methyl headgroup order at all the interfaces. If we only compare the results of the silane−PDMS mixtures without MVS, the SFG Fermi resonance signals from silane methyl headgroup of the γ-GPES−PDMS mixture before and after curing exhibit the biggest intensity change. This SFG signal intensity change is 4.68 − 1.85 = 2.83. For the γ-GPDES−PDMS mixture sample before and after curing, the SFG intensity change is 2.53 − 0.90 = 1.63, which is smaller than the previous γ-GPES−PDMS mixture case. For the γ-GPDMES−PDMS mixture, the SFG Fermi resonance signal intensity (at 2930 cm^{-1}) before curing is 0 and after curing is 1.58. Therefore, the difference is 1.58 − 0 = 1.58, which is the smallest among all the three cases. If we characterize the interfacial methyl ordering using the SFG signal strength of the

dx.doi.org/10.1021/la3041727 | Langmuir 2013, 29, 610−619

Table 4. Fermi Resonance Signal Strength Differences for Silanes before and after Curing As Well As with and without MVS; Correlated Adhesion Strengths Are Shown in the Right Column

variable	silanes	signal strength difference (Fermi resonance)	adhesion strength (MPa)
curing (cured)−(uncured)	γ-GPES	4.68 − 1.85 = 2.83	0.64 ± 0.02
	γ-GPDES	2.53 − 0.90 = 1.63	0.39 ± 0.02
	γ-GPDMES	1.58 − 0.00 = 1.58	0.24 ± 0.05
	γ-GPES:MVS	2.55 − 1.04 = 1.51	1.21 ± 0.15
	γ-GPDES:MVS	1.42 − 0.00 = 1.42	0.99 ± 0.12
	γ-GPDMES:MVS	0.82 − 0.00 = 0.82	0.92 ± 0.08
MVS (without MVS)−(with MVS) after curing	γ-GPES	4.68 − 2.55 = 2.13	1.21 ± 0.15
	γ-GPDES	2.53 − 1.42 = 1.11	0.99 ± 0.12
	γ-GPDMES	1.58 − 0.82 = 0.76	0.92 ± 0.08

methyl Fermi resonance signal, we can see that the more ethoxy headgroup the silane has, the stronger order it tends to have at the PET/uncured PDMS and PET/cured PDMS interfaces. In addition, the above discussion shows that the increases of the methyl interfacial ordering after curing PDMS follow the same trend. The adhesion results indicated that the γ-GPES−PDMS mixture tends to increase the adhesion of PDMS to PET, the γ-GPDES−PDMS mixture sample has similar adhesion as PDMS to PET, and the γ-GPDMES−PDMS mixture has weaker adhesion to PET than PDMS alone. Therefore, we believe that the ethoxysilane methyl headgroup ordering at the interfaces between PDMS−silane mixture and PET is related to adhesion. The improved adhesion is associated with better headgroup ordering or/and ordering change.

The addition of small amount of MVS to the PDMS−silane mixtures greatly changed the molecular structures at the interfaces. SFG signals of the ethoxy methyl group at the PET/uncured PDMS interfaces decreased for all the three silane cases. However, after curing PDMS, the ethoxy methyl group signals for all the three samples increased comparing to before curing, similar to the PDMS−silane mixture (without MVS) cases. After the curing process, the SFG methyl Fermi resonance signal strength change for the γ-GPES:MVS−PDMS mixture sample is 2.55 − 1.04 = 1.51, which is the biggest among the three samples (with MVS). The change for the γ-GPDES:MVS-PDMS mixture sample is 1.42 − 0 = 1.42, which is smaller than the previous case. For the γ-GPDMES:MVS-PDMS mixture, the change is 0.82 − 0 = 0.82, which is the smallest. The above observations are the similar to those discussed previously before the introduction of MVS to the samples. Again, the results indicate that the more ethoxy headgroups the silane has, the more order the ethoxy methyl group tends to have after curing, the larger ethoxy methyl ordering increase during the curing process. The γ-GPES:MVS-PDMS mixture sample has the strongest adhesion to PET, which is stronger than the γ-GPDES:MVS-PDMS sample, which in turn is stronger than the γ-GPDMES:MVS-PDMS mixture sample. Correlated to the SFG results, this again indicates that the silane headgroup ordering at the interfaces is related to adhesion. The better adhesion is also associated with better headgroup ordering or/and ordering change.

The curing process is a complicated chemical process that may involve multiple mechanisms. Although we find that the curing process can increase the order of silane methyl groups in ethoxy headgroup at the interfaces, it is still not clear if headgroup ordering at the interface directly resulted in good adhesion or the ordering is essential for some other mechanisms that eventually lead to good adhesion. Furthermore, the above observation cannot explain why MVS can greatly improve PDMS adhesion to PET while the samples with the addition of MVS exhibit weaker silane headgroup order at the interfaces. According to our previous publication on methoxysilane adhesion promoter,[55] the strong adhesion is related to the chemical reaction involving the silane methoxy headgroups at the interface. Therefore, it is necessary for silane methoxy headgroups to segregate to and order at the interface between PET and PDMS to have the interfacial chemical reaction for strong adhesion. It is the interfacial chemical reaction that leads to the decrease of SFG signals generated from the silane methoxy headgroup, resulting in strong adhesion. Therefore, the larger decrease of the SFG signals from methoxy groups after curing PDMS lead to stronger adhesion. However, this was opposite to what we observed in this study.

In this study, we have not observed methyl (in ethoxy headgroup) signal decrease after curing. Instead, such signals were found to increase after curing for ethoxysilanes. First of all, we observed that methyl groups (in ethoxy headgroup) of silanes with more ethoxy headgroups tend to order more at the PET/PDMS interface compared to those of silanes with less ethoxy headgroups. The stronger ethoxy ordering very likely involves more headgroup reaction at the interface. Therefore, the silane ordering is essential for good interfacial adhesion but not directly results in strong adhesion, since the interfacial reaction (which leads to the ethoxy signal decrease) is directly related to interfacial adhesion. Here when silanes were incorporated with PDMS without MVS, all samples showed headgroup ordering at the interface, but only γ-GPES improved the adhesion. γ-GPDES did not significantly improve adhesion although headgroups are ordered at the interface, while γ-GPDMES decreased the adhesion. Such results show that even though silane interfacial ordering provides headgroups needed for interfacial chemical reaction for strong adhesion, methyl ordering itself is not directly related to adhesion. With the addition of MVS into the system, methyl (in ethoxy group) signal decrease was not observed in this experiment. Instead, such signals increased for different systems with different increase amounts. This can be explained by different reactivity properties of ethoxysilanes and methoxysilanes. Curing can lead to more interfacial segregated silane headgroups; this will lead to SFG methyl signal increase. At the same time, curing can induce interfacial reactions involving silane headgroups, decreasing SFG methyl signals. These two effects may occur simultaneously in the curing process. For the methoxysilanes in previous study,[55] the silane headgroup reactivity is high, and therefore the interfacial methoxy groups decreased in number, resulting in SFG headgroup signal decrease after curing. It was well-known that ethoxysilanes reactivity is much less than methoxysilanes.[10] Accordingly, the interfacial reaction related headgroup signal decrease is less, resulting in total headgroup signal increase for ethoxysilanes compare to decrease for methoxysilanes. Less methyl SFG signal increase when MVS is coupled in the system indicates more chemical reactions involved, resulting in stronger adhesion.

Table 4 shows that with the addition of MVS to PDMS the SFG methyl signal increase is smaller compared to the cases

dx.doi.org/10.1021/la3041727 | Langmuir 2013, 29, 610−619

without MVS. Before and after curing, for the γ-GPES:MVS case, SFG signal strength change is 2.55 − 1.04 = 1.51, which is smaller compared to the γ-GPES case, which is 4.68 − 1.85 = 2.83. For the γ-GPDES:MVS case, the SFG signal strength change is 1.42 − 0 = 1.42, which is smaller compared to the γ-GPDES case: 2.53 − 0.90 = 1.63. For the γ-GPDMES:MVS case, the SFG signal change is 0.82 − 0 = 0.82, which is also smaller compared to 1.58 − 0 = 1.58 for γ-GPDMES without the addition of MVS. Such a difference likely indicates that MVS may have further induced chemical reaction of silane headgroup at the PET/PDMS interface and provides improved adhesion strength. The adhesion results shown in Figure 4 indicate that γ-GPES:MVS mixture results in the strongest adhesion at the PET/PDMS interface, while γ-GPDES:MVS mixture is the second, and the γ-GPDMES:MVS mixture leads to the weakest adhesion. But overall all the three mixtures have stronger adhesion than PDMS itself or PDMS incorporated with silanes alone. Considering all three samples with MVS, the bigger the difference in SFG headgroup signal before and after curing, the greater the adhesion the sample tends to have. The overall effect of MVS can also be compared only using the cured samples. The signal difference between γ-GPES and γ-GPES:MVS is 4.68 − 2.55 = 2.13, between γ-GPDES and γ-GPDES:MVS is 2.53 − 1.42 = 1.11, and between γ-GPDMES and γ-GPDMES:MVS is 1.58 − 0.82 = 0.76. It was shown that if only consider the presence and absence of MVS, the bigger signal difference also indicates the stronger the adhesion strength.

In the above discussion, we only considered the silane headgroup methyl Fermi resonance signal at 2930 cm^{-1}. This can avoid the possible complication caused by the symmetric and asymmetric C−H stretching signals contributed from Si−CH_3 groups in PDMS and MVS at ∼2900 and ∼2960 cm^{-1}. However, even if we take all three peaks into consideration, as shown in Table 3 (s) + (F) + (as), similar results can also be obtained. This indicates that possibly the contributions of PDMS and MVS are small or are similar for different samples.

The above discussion indicates that ethoxysilane headgroups tend to order at the interface between PET and PDMS, which is a key factor for the adhesion (as we discussed before). Silane headgroups can be involved in adhesion at the PET/PDMS interface similar to that at the silica/PDMS interface. Interfacial chemical reaction and entanglement that decrease the interfacial headgroup ordering (leading to the SFG signal decrease of the headgroups) can provide strong adhesion.

SUMMARY

Silane adhesion promoters are widely used to enhance PDMS adhesion to various substrates. Many of commonly used silanes can have negative environmental impact in the adhesion promoting process. In this study we focused on the study of environmental friendly ethoxysilanes. We compared three ethoxysilanes—γ-GPES, γ-GPDES, and γ-GPDMES—and these silane MVS 1:1 mixtures at the interfaces between silane or silane:MVS and PET, between uncured PDMS and PET, and between cured PDMS and PET. We find that different silanes tend to have different interfacial structures at the interfaces with PET. MVS can change the interfacial molecular interactions of silanes. We also find that addition of small amount of silane to PDMS can alter the interfacial molecular structures between PDMS and PET. The results show that silane headgroup order plays an important role in adhesion. The decrease of SFG headgroup signal indicates chemical reaction and disordering of such groups at the interfaces, which is related to improved adhesion. MVS tends to decrease the order of methyl group at the interfaces, which lead to much stronger adhesion. Together with previous publications, we demonstrated that silane headgroups greatly impact interfacial adhesion between PET and silicone elastomer.

AUTHOR INFORMATION

Corresponding Author

*E-mail zhanc@umich.edu.

Notes

The authors declare no competing financial interest.

ACKNOWLEDGMENTS

This work is supported by the University of Michigan and the Semiconductor Research Corporation (P13696). The authors want to thank Nick E. Shephard and Susan M. Rhodes from Dow Corning Corporation for their insightful suggestions on the project.

REFERENCES

(1) Kinloch, A. J. *Adhesion and Adhesives: Science and Technology*; Springer: Berlin, 1987.
(2) Charles, H. K. J. *Engineered Materials Handbook*; ASM International: Materials Park, OH, 1990; Vol. 3.
(3) Mittal, K. L. *Polymer Surface Modification: Relevance to Adhesion*; VSP: McCall, ID, 2004.
(4) Yacobi, B. G.; Martin, S.; Davis, K.; Hudson, A.; Hubert, M. Adhesive bonding in microelectronics and photonics. *J. Appl. Phys.* **2002**, *91*, 6227−6262.
(5) Mine, K.; Nishio, M.; Sumimura, S. Heat curable organopolysiloxane compositions containing adhesion additives. U.S. Patent 4033924, July 5, 1977.
(6) Schulz, J. R. Self-adhering silicone compositions and preparations thereof. U.S. Patent 4087585, May 2, 1978.
(7) Mittal, K. L. Interfacial chemistry and adhesion: recent developments and prospects. *Pure Appl. Chem.* **1980**, *52*, 1295−1305.
(8) Plueddemann, E. P. *Silane Coupling Agents*; Springer: Berlin, 1982.
(9) Sathyanarayana, M. N.; Yaseen, M. Role of promoters in improving adhesions of organic coatings to a substrate. *Prog. Org. Coat.* **1995**, *26*, 275−313.
(10) Hermanson, G. T. *Bioconjugate Techniques*; Academic Press: New York, 1996.
(11) Gray, T. E.; Lutz, M. A. Curable organopolysiloxane compositions with improved adhesion. U.S. Patent 5595826, Jan 21, 1997.
(12) Feresenbet, E.; Raghavan, D.; Holmes, G. A. The influence of silane coupling agent composition on the surface characterization of fiber and on fiber-matrix interfacial shear strength. *J. Adhes.* **2003**, *79*, 643−665.
(13) Mason, R.; Emerson, J.; Koberstein, J. T. Self-adhesion hysteresis in polydimethylsiloxane elastomers. *J. Adhes.* **2004**, *80*, 119−143.
(14) Kim, K. H.; Chaudhury, M. K. Shear-induced fracture at the interface of PDMS and a rigid slab modified with Polyelectrolyte Layers. *J. Adhes.* **2009**, *85*, 792−811.
(15) Chateauminois, A.; Fretigny, C.; Olanier, L. Friction and shear fracture of an adhesive contact under torsion. *Phys. Rev. E* **2010**, *81*, 026106.1−026106.12.
(16) Sakasegawa, D.; Tsuzuki, T.; Sugizaki, Y.; Goto, M.; Suzuki, A. Effects of degree of cross-links on adhesion curves of cross-linked polymers observed by a point-contact method. *Langmuir* **2010**, *26*, 5856−5863.
(17) Shen, Y. R. Surface properties probed by second-harmonic and sum-frequency generation. *Nature* **1989**, *337*, 519−525.

(18) Superfine, R.; Huang, J. Y.; Shen, Y. R. Nonlinear optical studies of the pure liquid/vapor interface: Vibrational spectra and polar ordering. *Phys. Rev. Lett.* **1991**, *66*, 1066−1069.
(19) Somorjai, G. A.; McCrea, K. R. Sum frequency generation: Surface vibrational spectroscopy studies of catalytic reactions on metal single-crystal surfaces. *Adv. Catal.* **2000**, *45*, 385−438.
(20) Chen, Z.; Shen, Y. R.; Somorjai, G. A. Studies of polymer surfaces by sum frequency generation vibrational spectroscopy. *Annu. Rev. Phys. Chem.* **2002**, *53*, 437−465.
(21) Johnson, C. M.; Tyrode, E.; Baldelli, S.; Rutland, M. W.; Leygraf, C. A vibrational sum frequency spectroscopy study of the liquid-gas interface of acetic acid-water mixtures: 1. Surface speciation. *J. Phys. Chem. B* **2005**, *109*, 321−328.
(22) Tyrode, E.; Johnson, C. M.; Baldelli, S.; Leygraf, C.; Rutland, M. W. A vibrational sum frequency spectroscopy study of the liquid-gas interface of acetic acid-water mixtures: 2. Orientation analysis. *J. Phys. Chem. B* **2005**, *109*, 329−341.
(23) Wang, J.; Chen, X.; Clarke, M. L.; Chen, Z. Detection of chiral sum frequency generation vibrational spectra of proteins and peptides at interfaces in situ. *Proc. Natl. Acad. Sci. U. S. A.* **2005**, *102*, 4978−4983.
(24) Baldelli, S. Surface structure at the ionic liquid-electrified metal interface. *Acc. Chem. Res.* **2008**, *41*, 421−431.
(25) Hirose, C.; Akamatsu, N.; Domen, K. Formulas for the analysis of surface sum-frequency generation spectrum by CH stretching modes of methyl and methylene groups. *J. Chem. Phys.* **1992**, *96*, 997−1004.
(26) Hirose, C.; Akamatsu, N.; Domen, K. Formulas for the analysis of the surface SFG spectrum and transformation coefficients of cartesian SFG tensor components. *Appl. Spectrosc.* **1992**, *46*, 1051−1072.
(27) Zhuang, X.; Miranda, P.; Kim, D.; Shen, Y. R. Mapping molecular orientation and conformation at interfaces by surface nonlinear optics. *Phys. Rev. B* **1999**, *59*, 12632−12640.
(28) Moad, A. J.; Simpson, G. J. A unified treatment of selection rules and symmetry relations for sum-frequency and second harmonic spectroscopies. *J. Phys. Chem. B* **2004**, *108*, 3548−3562.
(29) Lambert, A. G.; Davies, P. B.; Neivandt, D. J. Implementing the theory of sum frequency generation vibrational spectroscopy: A tutorial review. *Appl. Spectrosc. Rev.* **2005**, *40*, 103−145.
(30) Li, Q.; Kuo, C. W.; Yang, Z.; Chen, P.; Chou, K. C. Surface-enhanced IR−visible sum frequency generation vibrational spectroscopy. *Phys. Chem. Chem. Phys.* **2009**, *11*, 3436−3442.
(31) Wei, X.; Zhuang, X.; Hong, S. C.; Goto, T.; Shen, Y. R. Sum-frequency vibrational spectroscopic study of a rubbed polymer surface. *Phys. Rev. Lett.* **1999**, *82*, 4256−4259.
(32) Gracias, D. H.; Chen, Z.; Shen, Y. R.; Somorjai, G. A. Molecular characterization of polymer and polymer blend surfaces. Combined sum frequency generation surface vibrational spectroscopy and scanning force microscopy studies. *Acc. Chem. Res.* **1999**, *32*, 930−940.
(33) Chen, Z.; Ward, R.; Tian, Y.; Baldelli, S.; Opdahl, A.; Shen, Y. R.; Somorjai, G. A. Detection of hydrophobic end groups on polymer surfaces by sum-frequency generation vibrational spectroscopy. *J. Am. Chem. Soc.* **2000**, *122*, 10615−10620.
(34) Gautam, K. S.; Schwab, A. D.; Dhinojwala, A.; Zhang, D.; Dougal, S. M.; Yeganeh, M. S. Molecular structure of polystyrene at Air/Polymer and Solid/Polymer interfaces. *Phys. Rev. Lett.* **2000**, *85*, 3854−3857.
(35) Wang, J.; Chen, C.; Buck, S. M.; Chen, Z. Molecular Chemical Structure on Poly(methyl methacrylate) (PMMA) Surface Studied by Sum Frequency Generation (SFG) Vibrational Spectroscopy. *J. Phys. Chem. B* **2001**, *105*, 12118−12125.
(36) Ye, H.; Gu, Z.; Gracias, D. H. Kinetics of ultraviolet and plasma surface modification of poly(dimethylsiloxane) probed by sum frequency vibrational spectroscopy. *Langmuir* **2006**, *22*, 1863−1868.
(37) Lu, X.; Shephard, N.; Han, J.; Xue, G.; Chen, Z. Probing molecular structures of polymer/metal interfaces by sum frequency generation vibrational spectroscopy. *Macromolecules* **2008**, *41*, 8770−8777.
(38) Lu, X.; Li, D.; Kristalyn, C. B.; Han, J.; Shephard, N.; Rhodes, S.; Xue, G.; Chen, Z. Directly probing molecular ordering at the buried polymer/metal interface. *Macromolecules* **2009**, *42*, 9052−9057.
(39) Chen, Z. Investigating buried polymer interfaces using sum frequency generation vibrational spectroscopy. *Prog. Polym. Sci.* **2010**, *35*, 1376−1402.
(40) Ahn, D.; Dhinojwala, A. *Sum Frequency Generation Vibrational Spectroscopy of Silicone Surfaces & Interfaces*; Springer: Dordrecht, The Netherlands, 2012; pp 23−58.
(41) Hankett, J. M.; Zhang, C.; Chen, Z. Sum Frequency Generation and Coherent Anti-Stokes Raman Spectroscopic Studies on Plasma-Treated Plasticized Polyvinyl Chloride Films. *Langmuir* **2012**, *28*, 4654−4662.
(42) Zhang, C.; Hankett, J.; Chen, Z. Molecular level understanding of adhesion mechanisms at the epoxy/polymer interfaces. *ACS Appl. Mater. Interfaces* **2012**, *4*, 3730−3737.
(43) Du, Q.; Superfine, R.; Freysz, E.; Shen, Y. R. Vibrational spectroscopy of water at the vapor/water interface. *Phys. Rev. Lett.* **1993**, *70*, 2313−2316.
(44) Pieniazek, P. A.; Tainter, C. J.; Skinner, J. L. Interpretation of the water surface vibrational sum-frequency spectrum. *J. Chem. Phys.* **2011**, *135*, 044701.1−044701.12.
(45) Fu, L.; Wang, Z.; Yan, E. C. Y. Chiral vibrational structures of proteins at interfaces probed by sum frequency generation spectroscopy. *Int. J. Mol. Sci.* **2011**, *12*, 9404−9425.
(46) Boughton, A. P.; Yang, P.; Tesmer, V. M.; Ding, B.; Tesmer, J. J. G.; Chen, Z. Heterotrimeric G protein $\beta 1\gamma 2$ subunits change orientation upon complex formation with G protein-coupled receptor kinase 2 (GRK2) on a model membrane. *Proc. Natl. Acad. Sci. U. S. A.* **2011**, *108*, E667−E673.
(47) Liu, Y.; Jasensky, J.; Chen, Z. Molecular interactions of proteins and peptides at interfaces studied by sum frequency generation vibrational spectroscopy. *Langmuir* **2011**, *28*, 2113−2121.
(48) Wang, J.; Paszti, Z.; Mark, A.; Chen, Z. Measuring polymer surface ordering differences in air and water by sum frequency generation vibrational spectroscopy. *J. Am. Chem. Soc.* **2002**, *124*, 7016−7023.
(49) Chen, C. Y.; Wang, J.; Even, M. A.; Chen, Z. Sum frequency generation vibrational spectroscopy studies on "buried" polymer/polymer interfaces. *Macromolecules* **2002**, *35*, 8093−8097.
(50) Ye, S.; McClelland, A.; Majumdar, P.; Stafslien, S. J.; Daniels, J.; Chisholm, B.; Chen, Z. Detection of tethered biocide moiety segregation to silicone surface using sum frequency generation vibrational spectroscopy. *Langmuir* **2008**, *24*, 9686−9694.
(51) Ye, S.; Majumdar, P.; Chisholm, B.; Stafslien, S.; Chen, Z. Antifouling and antimicrobial mechanism of tethered quaternary ammonium salts in a cross-linked poly(dimethylsiloxane) matrix studied using sum frequency generation vibrational spectroscopy. *Langmuir* **2010**, *26*, 16455−16462.
(52) Loch, C. L.; Ahn, D.; Chen, Z. Sum frequency generation vibrational spectroscopic studies on a silane adhesion-promoting mixture at a polymer interface. *J. Phys. Chem. B* **2006**, *110*, 914−918.
(53) Loch, C. L.; Ahn, D.; Vazquez, A. V.; Chen, Z. Diffusion of one or more components of a silane adhesion-promoting mixture into poly(methyl methacrylate). *J. Colloid Interface Sci.* **2007**, *308*, 170−175.
(54) Vázquez, A. V.; Shephard, N. E.; Steinecker, C. L.; Ahn, D.; Spanninga, S.; Chen, Z. Understanding molecular structures of silanes at buried polymer interfaces using sum frequency generation vibrational spectroscopy and relating interfacial structures to polymer adhesion. *J. Colloid Interface Sci.* **2009**, *331*, 408−416.
(55) Zhang, C.; Shephard, N. E.; Rhodes, S. M.; Chen, Z. Headgroup effect on silane structures at buried polymer/silane and polymer/polymer interfaces and their relations to adhesion. *Langmuir* **2012**, *28*, 6052−6059.
(56) Bluemel, J. Reactions of ethoxysilanes with silica: A solid-state NMR study. *J. Am. Chem. Soc.* **1995**, *117*, 2112−2113.

(57) Zhang, C.; Wang, J.; Khmaladze, A.; Liu, Y.; Ding, B.; Jasensky, J.; Chen, Z. Examining surface and bulk structures using combined nonlinear vibrational spectroscopies. *Opt. Lett.* **2011**, *36*, 2272−2274.
(58) Witucki, G. L. A silane primer: chemistry and applications of alkoxy silanes. *J. Coat. Technol.* **1993**, *65*, 57−60.